SNR-dependent Filter Design for Improving Depth of Field Using Modified Least Squares

Geng-Shi Jeng and Sheng-Wen Huang

Department of Electrical Engineering, National Taiwan University, Taipei, Taiwan, R. O. C.

Abstract—Conventional ultrasound systems with fixed transmit and dynamic receive focusing suffer from limited depth of field and poor SNR uniformity. Based on fixed receive focusing, this paper proposes an SNR-dependent 2-D retrospective filtering technique to extend the depth of field, in which both the sidelobe energy and the filter energy are minimized simultaneously. According to the estimated SNR of the unfiltered image, the proposed 2-D filter can provide the optimal compromise between image quality and SNR while maintaining a moderate filter size. Simulations were performed to demonstrate the efficacy of the proposed technique. It has been shown that the proposed 2-D filter technique outperforms conventional 1-D lateral filter and classical 2-D Wiener filter in terms of both SNR and contrast resolution.

I. INTRODUCTION

Most ultrasound imaging systems use fixed transmit and dynamic receive focusing. When the region of interest is away from the focus, the image quality often degrades gradually and thus depth of field (DOF) is limited. Ideally, the pulse-echo beam characteristics should not change with range. Additionally, SNR along the range is also required to maintain at an acceptable level to assure good uniformity of the image quality.

DOF can be extended by filtering the post-beamformed data [1], [2]. This method is attractive for its simplicity. Freeman *et al.* proposed a depth-dependent lateral filtering to synthesize the dynamic transmit focus retrospectively [1]. Further, Li *et al*. [2] applied 1-D filtering to a more simplified beamformer based on fixed receive focusing. Despite the hardware simplicity, 1-D lateral filtering has limited performance due to the filtering being applied only in one direction. Moreover, both schemes use least-squares (LS) approach in which the desired function is required. Consequently, the designed filter may behave as an inverse filter that only works well when SNR is sufficiently high.

In this paper, we will extend the 1-D filtering approach to 2-D. With a 2-D filter, the filter length can be increased without requiring a large number of scan lines. With this advantage, the filter performance can still maintain at low SNR.

2-D deconvolution methods have also been proposed to restore the resolution on post-detection images [3], [4]. Most of the deconvolution filters in this case are implemented as a Wiener filter. Although the Wiener filter succeeds in improving spatial resolution, it fails to suppress near sidelobes and makes contrast resolution worse than the proposed 2-D filter, as will be shown latter.

Based on the simple fixed receive focusing architecture, this paper extends 1-D filtering to 2-D filtering, and takes SNR into account while designing 2-D filters. Specifically, the conventional LS approach is modified so that the desired function is no longer needed and the SNR is taken into account.

II. METHODS

Assuming linearity and spatial shift-invariance, a B-mode image formed by fixed transmit and receive focusing can be expressed as the sum of the following two terms: the convolution between the defocused point spread function (PSF) and the tissue response, and the uncorrelated noise. Conceptually, if the defocused PSF is known *a priori*, a retrospective filter can be applied to deconvolve the defocused PSF. Hence, the goal for our filter design is to make the filtered defocused PSF as narrow as possible while not amplifying the noise.

Fig.1 illustrates how the filter with a size of $K \times L$ is convolved with the defocused PSF. The convolution is performed within the truncated area with a size of $M \times N$. A 2-D filter is 180° rotated first, and then acts as a moving window row-by-row from the upper-left to the lower-right corner. The area within the inner dashed circle (-20dB contour of the in-focus PSF) is defined as the mainlobe region. The proposed filter

technique aims to simultaneously minimize the sidelobe and filter energy, subject to an equality constraint. Hence, the objective function can be expressed in a Lagrange form as

$$C = \alpha \boldsymbol{f}^{\mathrm{H}} \boldsymbol{Q} \boldsymbol{f} + (1-\alpha) \boldsymbol{f}^{\mathrm{H}} \boldsymbol{I} \boldsymbol{f} - \lambda^{\mathrm{H}} (\boldsymbol{A}_{\mathrm{e}} \boldsymbol{f} - \boldsymbol{b}_{\mathrm{e}}), \qquad (1)$$

where $\boldsymbol{f} = [f_{K,L} \quad f_{K,L-1} \quad \cdots \quad f_{1,2} \quad f_{1,1}]^{\mathrm{T}}$ is the filter to be designed (in a reshaped vector form), $\boldsymbol{I}$ is a $KL \times KL$ identity matrix, $\boldsymbol{f}^{\mathrm{H}} \boldsymbol{Q} \boldsymbol{f}$ denotes the sidelobe energy and $\boldsymbol{f}^{\mathrm{H}} \boldsymbol{I} \boldsymbol{f}$ denotes the filter energy, α is the weighting, $\boldsymbol{b}_{\mathrm{e}} = 1$, and the vector $\boldsymbol{A}_{\mathrm{e}}$ is defined such that the product $\boldsymbol{A}_{\mathrm{e}} \boldsymbol{f}$ is the filtered result at the range intended to be focused, as indicated as '$\oplus$' in Fig. 1. The optimal filter $\boldsymbol{f}_{\mathrm{opt}}$ for (1) is

$$\boldsymbol{f}_{\mathrm{opt}} = \boldsymbol{P}^{-1} \boldsymbol{A}_{\mathrm{e}}^{\mathrm{H}} (\boldsymbol{A}_{\mathrm{e}} \boldsymbol{P}^{-1} \boldsymbol{A}_{\mathrm{e}}^{\mathrm{H}})^{-1} \boldsymbol{b}_{\mathrm{e}}, \qquad (2)$$

where $\boldsymbol{P} = \alpha \boldsymbol{Q} + (1-\alpha) \boldsymbol{I}$. To understand the effect of minimizing the filter energy on the resultant SNR, consider the case in which a white noise with zero mean and variance σ_w^2 is superimposed on the defocused PSF. The ensemble average of the sidelobe energy E of this "noisy" filtered PSF is

$$E = \boldsymbol{f}^{\mathrm{H}} \boldsymbol{Q} \boldsymbol{f} + D \sigma_w^2 \boldsymbol{f}^{\mathrm{H}} \boldsymbol{I} \boldsymbol{f}, \qquad (3)$$

where D is the number of points in the sidelobe region. The second term in (3) represents the noise energy in the sidelobe region. Comparing (1) to (3), it is straightforward that minimizing the filter energy enables the noise to be taken into account. Furthermore, α is uniquely determined by D and σ_w^2 given a specific defocused PSF. Note that the above approach can also be applied to 1-D filtering. Nonetheless, the 2-D filtering approach proposed in this paper has the advantage of extending the filter length without using a large number of scan lines.

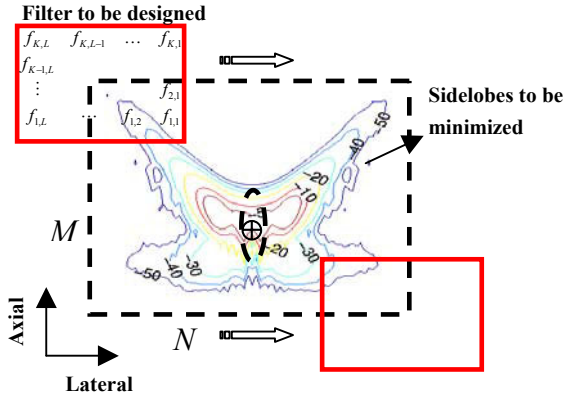

Fig. 1. Schematic description of the design method for the proposed filter technique.

III. SNR-DEPENDENT CHARACTERISTICS OF THE PROPOSED FILTER

Simulations using Field II [5] were conducted to investigate the SNR-dependent property of the proposed filtering technique. A 128-element, 3.5-MHz/40% array with a pitch of 0.22 mm was used. The transmit and receive focal points are 60mm. Baseband beamforming was applied. The above simulation parameters were used throughout this paper.

Points placed at different ranges were imaged to obtain the corresponding defocused PSFs. For each PSF, the optimal filters were derived according to (2) by varying α from 0 to 1. For each α, the peak power was calculated by applying the optimal filter whose energy was normalized to unity to the defocused PSF. To evaluate the sidelobe energy in the presence of noise, the optimal filter for each α was directly applied to (3) where a noise variance was specified. The result obtained (e.g., E) was then divided by D, which can be regarded as the average sidelobe energy of the "noisy" filtered PSF. Fig. 2 shows the relationship between output SNR, defined as the ratio of the peak power of filtered PSF to the noise variance, and average sidelobe energy at ranges of 120 mm and 40 mm. Three different filters, including 1-D, 2-D, and Wiener filters, were compared. Here, 1-D filter has the same lateral size as 2-D filter but only with one axial tap. The Wiener filter is implemented in the frequency domain and has a form of $H^*(\omega,\mu) / |H(\omega,\mu)|^2 + \nu$, where $H(\omega,\mu)$ is 2-D Fourier transform of the defocused PSF and ν denotes the variance ratio of noise to signal and is usually set as a constant. To ease improper truncation when the Wiener filter was applied, the unfiltered PSF had been zero-padded before Fourier transform, resulting in double the length in both axial and lateral directions. For both plots shown in Fig. 2, 2-D filter size is 35 (lateral) by 11(axial) and Wiener filter size is 161 by 61. Input SNR, defined as SNR before filtering, is assumed to be 23.82 dB at 120 mm and 42.14 dB at 40 mm.

As shown in Fig. 2, a turning point corresponding to the minimum average sidelobe energy can be found on each curve. Note that the turning points for 1-D filter do exist but are not clearly seen due to the display scale. The turning points shown here suggest the lowest average sidelobe energy in a noisy environment. Also, these turning points adapt themselves to different input SNRs. Among these three filters, 2-D filter is superior in that its turning point has not only the

lowest sidelobes but also a high output SNR. In comparison, the turning point (marked as asterisk) for the Wiener filter is not apparent and thus is not a good compromise. Note that the point corresponding to classical MSE-based Wiener filter (marked as cross) is located on the left side of its own turning point.

As also suggested in Fig. 2, under different input SNR, there always exists an optimal α in determining the filter coefficients. To build the relationship between the optimal α and input SNR, we varied input SNR (or noise variance) in (3), applied the filters with different α derived in (2) to (3), and found the optimal α minimizing the "noisy" sidelobe energy (e.g. E). Fig. 3 shows such relationships evaluated at 120 mm, 80 mm and 40 mm. As expected, α increases as input SNR increases.

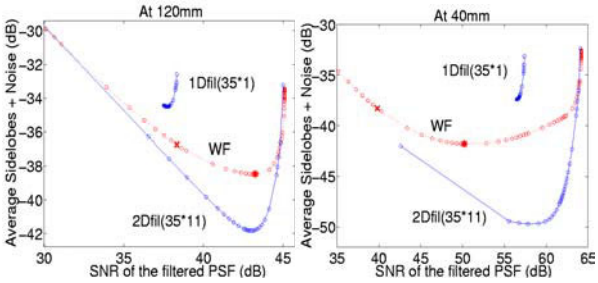

Fig. 2. Relationship between output SNR and average sidelobe energy of the "noisy" filtered PSF at 120 mm (left) and 40 mm (right).

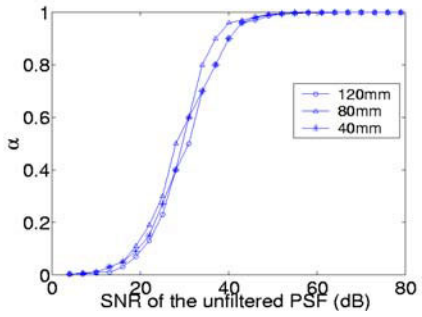

Fig. 3. Optimal α versus input SNR.

Accordingly, an SNR-dependent filtering can be achieved. For this purpose, before filtering, a filter set consisting of filters with α from 0 to 1 is constructed first. Then, SNR of the unfiltered image is evaluated according to an autocorrelation method [3]. Finally, a proper filter is selected out of the filter set by examining the relationship between input SNR and α.

IV. SIMULATION RESULTS

Point targets and anechoic cysts were simulated based on fixed receive focusing (FixRx) to investigate the validity of the proposed method. As comparisons, two images were also formed by dynamic transmit and receive focusing (DynTxRx) and only dynamic receive focusing (DynRx).

A. Point Targets

Nine point targets were placed at on-axis ranges from 40 mm to 120 mm with a spacing of 10 mm. Before filtering, the image was equally divided into nine zones. For each zone, the 2-D filter set as a function of α was constructed. Next, random noises were inserted into the raw data so that SNR at the focal point (i.e., 60 mm) was 60 dB. After estimating the input SNR in each zone, a proper 2-D filter was chosen and then applied to the whole zone. The 2-D filter sizes and the corresponding α at different ranges are listed in Table I. By comparison, Wiener filters with a size of 461 by 133 were also applied according to input SNR. Fig. 4(a)–(c) show 50 dB images before scan conversion for DynTxRx, DynRx, and FixRx, respectively. Note that each point target is individually normalized to its maximum. Applying 1-D, 2-D, and Wiener filters to the image for FixRx resulted in the image shown in Fig. 4(d)–(f), respectively. Clearly, compared to the original FixRx image, the image quality for all filters is improved. Specifically, the image quality of 2-D filter is comparable to that for DynTxRx with an exception of reduced SNR in deep ranges. Comparing (e) to (f), SNR improvements for 2-D and Wiener filters are similar. However, for Wiener filtering, large near sidelobes arise greatly around each point target.

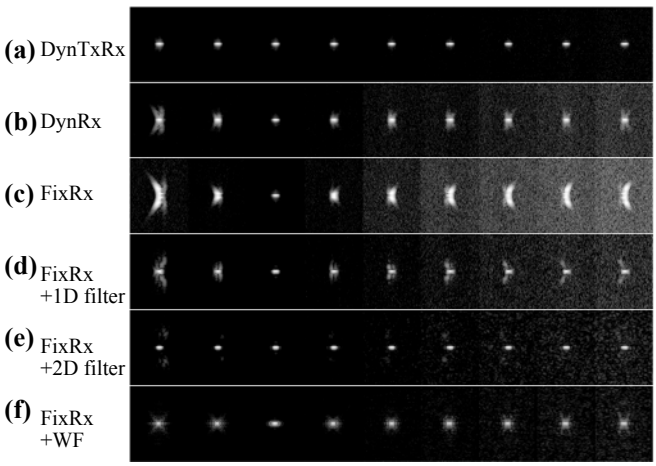

Fig. 4. 50 dB point target images before scan conversion. The horizontal axis is the depth from 35 mm (left) to 125 mm (right) and the vertical axis is azimuth.

B. Anechoic Cysts

A collection of random scatterers is distributed in an area with a size of 30 mm (lateral) by 12 mm (axial), in which there is an anechoic cyst with a radius of 4 mm and centered at 120 mm. Random noises were imposed in the raw data so that the SNR of the whole scattering region was 30 dB. The filter with $\alpha = 0.5$ corresponding to 120 mm was applied to the overall image (see Fig. 3).

Fig. 5 shows 30 dB images in the same order as Fig. 4. Note that panel (f) shows Wiener filtered image with the best CNR (will be defined later). All filters make the cyst more visible. In particular, the 2-D filtered image quality is better than 1-D and Wiener filtered images. Panel (f) illustrates the large sidelobe problem associated with Wiener filtering, where the spatial resolution is improved but the cyst is disrupted by sidelobes.

As a quantitative comparison, contrast-to-noise ratio (CNR) was evaluated according to the following definition: $|\mu_b - \mu_c| / \sqrt{0.5(\sigma_b^2 + \sigma_c^2)}$, where μ_b and σ_b^2 denote the mean and variance of intensity in the speckle background (marked as the left-hand white box in Fig. 5(a)), respectively, μ_c represents the mean intensity of the cyst (marked as the central white box), and σ_c^2 is its variance. For all images shown in Fig. 5, CNR, as well as SNR computed in the area indicated as the right-hand black box, were listed together in Table II. Specifically, SNR after 2-D filtering is higher than 1-D filtering by a factor of close to 4 dB.

V. CONCLUSIONS

In this paper, an SNR-dependent 2-D filter was proposed with the potentials of extending DOF and maintaining the SNR uniformity. By estimating SNR of the unfiltered image, the proposed filter method provides a compromise between the quality of PSF and the resultant SNR. Simulation results demonstrate the proposed 2-D filter performs better than the 1-D lateral filter and the classical 2-D Wiener filter. Furthermore, unlike the FFT-based Wiener filter implemented with a very large filter size, the proposed filter technique performs linear convolution and maintains a moderate filter size. Since only fixed focusing is required, the beam-former can be greatly simplified. The system thus requires a large memory to store the filter sets and a real-time implementation to perform the 2-D filtering.

TABLE I. Filter Sizes And The Optimal α Along The Range

Depth (mm)	40	50	60	70	80	90	100	110	120
Lateral size	35	25	9	25	29	29	29	31	35
Axial size	11	11	7	11	11	11	11	11	11
α	0.96	0.98	0.99	0.96	0.8	0.6	0.4	0.25	0.19

ACKLOWLEDGEMENTS

The authors would like to thank Dr. Pai-Chi Li for his considerable assistance.

REFERENCES

[1] S. Freeman *et al.,* "Retrospective dynamic transmit focusing," *Ultrason. Imag.*, vol. 17, pp. 173-196, 1995.

[2] M.-L. Li and P.-C. Li, "Filter-based synthetic transmit and receive focusing," *Ultrason. Imag.*, vol. 23, pp. 73-89, 2001.

[3] J. A. Jensen *et al.*, "Deconvolution of *in vivo* B-mode ultrasound images," *Ultrason. Imag.*, vol. 15, pp. 122-133, 1993.

[4] T. Taxt, "Restoration of medical ultrasound images using two-dimensional homomorphic deconvolution," *IEEE Trans. UFFC*, vol. 42, pp. 543-554, 1995.

[5] J. A. Jensen, "Field: A program for simulating ultrasound systems," *Med. Biol. Eng. Comput.*, vol. 34, pp. 351-359, 1996.

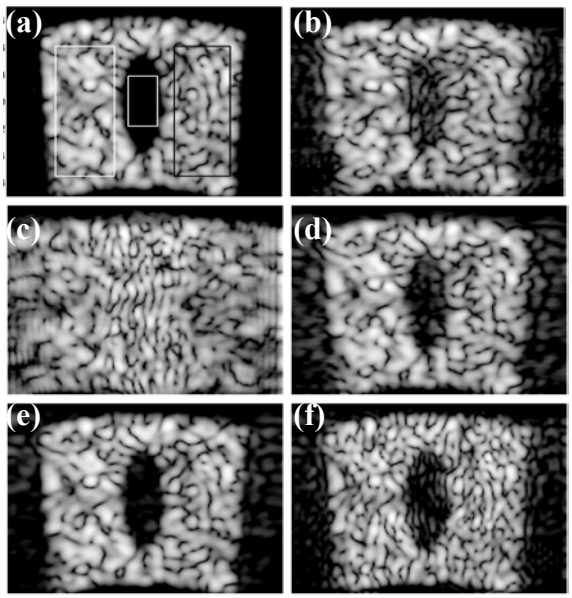

Fig. 5. 30 dB cyst images before scan conversion. The horizontal and vertical axis are azimuth and range, respectively. The order of plots is the same as Fig. 4.

TABLE II. CNR And SNR Evaluations In Fig. 5

	CNR	SNR (dB)
(a) DynTxRx	5.48	41.28
(b) DynRx	2.25	30.43
(c) FixRx	0.15	29.35
(d) FixRx+1Dfilter	3.17	30.93
(e) FixRx+2Dfilter	3.88	34.69
(f) FixRx+WF	2.78	35.19